Available online at www.sciencedirect.com
SCIENCE DIRECT®
Inorganica Chimica Acta 358 (2005) 3311–3319
Inorganica Chimica Acta
www.elsevier.com/locate/ica

Experimental and DFT studies on the DNA-binding trend and spectral properties of complexes $[Ru(bpy)_2L]^{2+}$ (L = dmdpq, dpq, and dcdpq)

Xue W. Liu [a], Jun Li [a], Hong Deng [a], Kang C. Zheng [a,*], Zong W. Mao [a], Liang N. Ji [a,b,*]

[a] Department of Chemistry, School of Chemistry and Chemical Engineering, Zhongshan (Sun Yat-Sen) University, Xingang Street, Guangzhou 510275, PR China

[b] The key Laboratory of Gene Engineering of Ministry of Education, Zhongshan (Sun Yat-Sen) University, Guangzhou 510275, PR China

Received 22 September 2004; received in revised form 25 April 2005; accepted 5 May 2005
Available online 27 June 2005

Abstract

The trend in DNA-binding affinities and the spectral properties of a series of Ru(II) polypyridyl complexes, $[Ru(bpy)_2(dmdpq)]^{2+}$ (**1**), $[Ru(bpy)_2(dpq)]^{2+}$ (**2**), $[Ru(bpy)_2(cndpq)]^{2+}$ (**3**) (bpy = 2,2′-bipyridine; dpq = dipyrido[3,2-d:2′,3′-f]quinoxaline; dmdpq = dimethyl-dpq; dcdpq = di-cyano-dpq), have been experimentally and theoretically investigated. The DNA-binding constants K_b of the complexes were determined systematically with spectrophotometric titration. The density functional theory (DFT) and time-dependent DFT (TDDFT) calculations were carried out for these complexes. The experimental results show that these complexes bind to DNA in intercalation mode, and the order of their intrinsic DNA-binding constants K_b is $K_b(\mathbf{1}) < K_b(\mathbf{2}) \ll K_b(\mathbf{3})$. The substituents on the intercalative ligands of the complexes play a very important role in the control of DNA-binding affinities of the complexes, in particular, the stronger electron-withdrawing substituent (–CN) on the intercalative ligand can greatly improve the DNA-binding property of the derivative complex. The trend in DNA-binding affinities as well as the spectral properties of metal–ligand charge-transition (^{1}MLCT) of this series of complexes can be reasonably explained by applying the DFT and TDDFT calculations and the frontier molecular orbital theory.

Keywords: Ru(II) complex; DNA-binding; Spectral property; Intercalation mode; DFT calculation

1. Introduction

The trends in DNA-binding of transition metal complexes, especially Ru(II) polypyridyl complexes and the related behaviors have aroused a great deal of interests of many researchers [1–8]. Clarification of these trends will be very helpful for the comprehension and the control of interactions between the complexes and DNA, and thus for the comprehension of mechanisms of DNA mutation and damage, as well as the design of new clinic anti-cancer drugs and novel complexes with biochemical activity [1,2,5].

At present, a considerable number of Ru(II) polypyridyl complexes have been synthesized and characterized, and the DNA-binding properties of the complexes have been investigated with spectrophotometric titration, viscosity measurements, equilibrium dialysis and circular dichroism spectroscopy [9–15]. Three types of binding modes, i.e., electrostatic binding mode, groove binding mode and intercalative binding mode, for the interaction mechanism between metal complexes and DNA have

* Corresponding authors. Tel.: +86 20 84110696; fax: +86 20 84035497.
E-mail addresses: ceszkc@zsu.edu.cn (K.C. Zheng), cesjln@zsu.edu.cn (L.N. Ji).

0020-1693/$ - see front matter © 2005 Elsevier B.V. All rights reserved.
doi:10.1016/j.ica.2005.05.006

been proposed and further developed [16–18]. Since many important applications of these complexes, e.g., DNA-structural probe [2], molecular "light switch" [15], and DNA-photocleavage reagent [2,9], require that the complexes bind to DNA in an intercalation mode, so much work has been focused on the prototypes $[Ru(bpy)_2L]^{2+}$ or $[Ru(phen)_2L]^{2+}$ with symmetric intercalative aromatic ligand (L), such as dipyrido [3,2-d:2′,3′-f]quinoxaline (dpq), dipyrido[3,2-a:2′,3′-c]phenazine (dppz), 2-phenylimidazo[4,5-f][1,10]-phenanthroline (pip) and their substituent derivatives [1,2,17]. In order to guide the design and synthesis of new complexes with excellent bioactivity, some important factors affecting DNA-binding affinities of such a kind of Ru(II) polypyridyl complexes, e.g., the planarity and planarity area (*S*) and substituent properties of the intercalative ligands, as well as ancillary ligand effects, have been experimentally summarized in certain scale [2,17].

In addition to the experimental studies, the transition metal polypyridyl complexes have also attracted many theoretical chemists. Various theoretical researchers have been trying to correlate some theoretical predictions to the experimental findings. In particular, more and more computations applying the density functional theory (DFT) [19–22] and the time-dependent DFT (TDDFT) methods [23–26] have been reported [27–37], because the DFT method can better consider electron correlation energies and obviously reduce the computation expenses. Furthermore, TDDFT method can suit the calculations of such a kind of complexes for their excited states, especially for their spectral properties. However, when quantum-chemical computations are applied to inorganic biochemical field, up to now, the supramolecular system formed from DNA and a metal complex is too large in size to be calculated yet. Therefore, it is very important and necessary to theoretically analyze the interaction between the complexes and DNA from their individual electronic structural characteristics and explore the trend in the DNA-binding affinities of complexes and the related behaviors. In this field, the molecular orbital theory, in particular, the frontier molecular orbital theory introduced by Fukui et al. [38] and Fleming [39] will play an important role. Recently, Rillema et al. [35] reported the results on Ru(II) two ring diimine complex cations with the DFT method and suggested that the lowest energy transitions are metal-to-ligand charge transfer and that the LUMO of the mixed ligand complex $[RuL_1L_2L_3]^{2+}$ is mainly located on the ligand with the lowest LUMO energy in the corresponding complex $[RuL_3]^{2+}$ with homogeneous ligand ($L = L_1$ or L_2 or L_3), based on the distributions of HOMOs and LUMOs of the complexes. Via investigating the energies of frontier molecular orbitals, Reha et al. [36] reported some valuable results as follows: all intercalators, such as ethidium and so on, are good electron acceptors because their LUMO energies are negative, all bases and base pairs of isolated DNA, e.g., adenine, thymine, whereas adenine-thymine (AT), etc., are all good electron donors and very poor electron acceptors because their LUMO energies are all positive in contrast to negative LUMO energies of intercalators. Kurita and Kobayashi [37] reported the density functional MO calculations for stacked DNA base-pair model with backbones and the results that the energies of the HOMO and occupied MO near HOMO are rather high and their components are mainly distributed on the base-pairs of DNA. Therefore, Kurita's results offered a further theoretical foundation for the base-pairs of DNA being good electron donors. We have also reported some DFT results on the electronic structures and related properties of some Ru(II) polypyridyl complexes, e.g., $[Ru(bpy)_2(6,6'\text{-}2R\text{-}dpq)]^{2+}$ (R = OH, H and F), $[Ru(phen)_2(9,9'\text{-}2R\text{-}dpq)]^{2+}$ ($R = NH_2$, OH, H and F), $[Ru(bpy)_2L]^{2+}$ (L = *o*-hpip, *m*-hpip and *p*-hpip), $[Ru(phen)_2(p\text{-}L)]^{2+}$ (L = mopip, hpip and npip), etc. [9,40–43]. These theoretical efforts on the level of molecular electronic structures of the complexes and DNA are very significant in guiding experimental works.

In this paper, the trend in DNA-binding affinities and the spectral properties of a series of Ru(II) polypyridyl complexes $[Ru(bpy)_2L]^{2+}$ (L = dmdpq, dpq, and dcdpq), i.e., $[Ru(bpy)_2(6,6'\text{-}2R\text{-}dpq)]^{2+}$ ($R = CH_3$, H, CN), were experimentally and theoretically studied. The DNA-binding constants K_b of the complexes were determined systematically with spectrophotometric titration. The theoretical calculations were performed by applying the DFT and TDDFT methods. This paper is mainly focused on experimentally revealing the trend in DNA-binding affinities of such a type of Ru(II) polypyridyl complexes and on theoretically attempting to understand them in order to effectively control the DNA-binding affinities of the complexes by selecting some suitable substituents. In addition, the spectral properties of ^{1}MLCT of this series of complexes were further studied by applying the TDDFT calculations.

2. Experimental

2.1. Synthesis and characterization

The synthesis, purification and characterization of all complexes were performed according to the literature procedures [44–46]. The related spectral properties of the complexes are given in Table 1.

2.2. Binding constant measurements

Interactions of complexes with calf thymus DNA have been studied by NMR spectra, electronic absorption spectra, CD spectra, cyclic voltammetry, steady-state fluorescence spectra, and viscosity measurements.

Table 1
Absorption and emission spectra, and DNA-binding constants K_b of $[Ru(bpy)_2L]^{2+}$

Complex	Absorption λ_{max} (nm)				K_b (M^{-1})	Emission λ_{max} (nm)			
	Free	Bound	$\Delta\lambda$	$H\%$		Free	Bound	$\Delta\lambda$	I/I_0
1 $[Ru(bpy)_2dmdpq]^{2+}$	453	453	0	−11	2.3×10^4	607	603	−4	2.7
2 $[Ru(bpy)_2dpq]^{2+}$	453	458	5	−14	4.7×10^4	629	625	−4	3.2
3 $[Ru(bpy)_2dcdpq]^{2+}$	450	452	2	−20	3.9×10^5	588	582	−6	20.7

Some results have been reported by us [44,47], and the results show that these complexes bind to DNA in intercalation mode, but their binding constants K_b have not been reported before. In order to explore the trend in DNA-binding affinities and the related behaviors of the complexes, the binding constants K_b of the complexes were further studied and determined systematically according to Eq. (1) [48], through a plot of [DNA]/($\varepsilon_a - \varepsilon_f$) versus [DNA]

$$\frac{[DNA]}{\varepsilon_a - \varepsilon_f} = \frac{[DNA]}{\varepsilon_b - \varepsilon_f} + \frac{1}{K_b(\varepsilon_b - \varepsilon_f)} \quad (1)$$

where [DNA] is the concentration of DNA in base pairs, ε_a, ε_f and ε_b are, respectively, the apparent extinction coefficient (A_{obs}/[M]), the extinction coefficient for free metal (M) complex and the extinction coefficient for the metal (M) complex in the fully bound form. In plots of [DNA]/($\varepsilon_a - \varepsilon_f$) versus [DNA], K_b is given by the ratio of slope to intercept (see Fig. 2).

3. Computational

Structural schematic diagram of the complexes is shown in Fig. 1. Every octahedral complex $[Ru(bpy)_2L]^{2+}$ (L = dmdpq, dpq, and dcdpq), i.e., $[Ru(bpy)_2(6,6'\text{-}2R\text{-}dpq)]^{2+}$ (R = CH_3, H and CN), forms from Ru(II) ion and an intercalative ligand (L) called main ligand, and two bpy ligands called co-ligand.

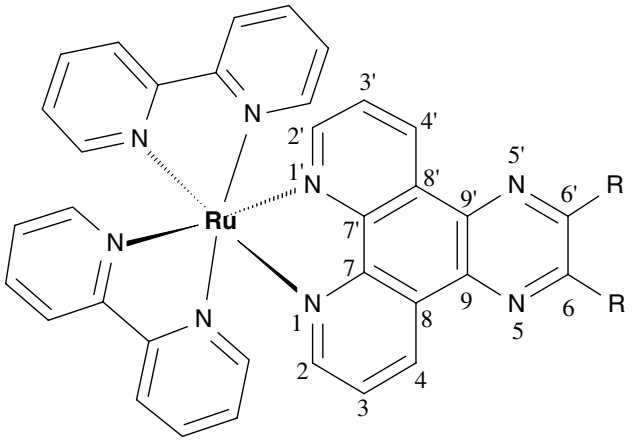

Fig. 1. Structural schematic diagram of $[Ru(bpy)_2L]^{2+}$ (L = dmdpq, dpq, and dcdpq).

These complexes all belong to C_2 symmetry. All calculations have been performed with the GAUSSIAN-98 quantum chemistry program-package [49]. The ground state structures were optimized at the DFT/B3LYP level using 6-31G* basis set on the carbon, nitrogen, and hydrogen atoms and LanL2DZ pseudo-potential [22,50,51] on the ruthenium atom. The full geometry optimization computations for the ground states of these complexes with singlet state [52] were carried out. The gas-phase singlet-excited-state energies were calculated by the TDDFT method based on the ground state geometries of the complexes. In order to vividly depict the detail of the frontier molecular orbitals, the stereo-contour graphs of some related frontier molecular orbitals of the complexes for the ground states were also drawn with the MOLDEN v3.7 program [53].

4. Results and discussion

4.1. Computed geometric structures of the complexes

The computed selective bond lengths and bond angles of this series of complexes and their parent complex $[Ru(bpy)_3]^{2+}$ for comparison are all shown in Table 2.

From Table 2, we can see that the substituents have slight effects on geometric structures of the complexes. Here, π-electron-withdrawing group (–CN) makes the coordination bond-length of main ligand (Ru–N_m) a little longer than that of co-ligand, although substituent effects on whole geometrical structures of the complexes are just only slight.

Comparing the computed results of the parent complex $[Ru(bpy)_3]^{2+}$ [52] with its experimental data (see in Table 2), we can find that the computed coordination bond lengths (Ru–N) are greater than those of the experiments by ~3%, and the computed coordination bond angles (A) are less than those of the experiments by ~1%. At the same time, the computed mean bond-lengths C–C (and C–N) of the ligand skeletons of these complexes are very close to their general bond-length (0.140 nm). Although the direct comparison between the computed results and the corresponding experimental values for each of the substitution derivatives was not performed because the reports on their crystal structures have not been found yet, the results of the full geometry optimization computations by the DFT method should

Table 2
Computed selective bond lengths (nm) and bond angles (°) of $[Ru(bpy)_2L]^{2+}$ and $[Ru(bpy)_3]^{2+}$ for comparison

Complex (calc.)	$M–N_m$[a]	$M–N_{co}$	A_m[b]	A_{co}	$C–C_m$	$C–C_{co}$	$C–X_m$
					$C–N_m$[c]	$C–N_{co}$[d]	X = –CH_3, –CN
0 $[Ru(bpy)_3]^{2+}$	0.2118	0.2118	77.6	77.6	0.1381	0.1381	–
$[Ru(bpy)_3]^{2+}$ (expt.)	0.2056	0.2056	78.7	78.7	0.1369	0.1369	–
1 $[Ru(bpy)_2dmdpq]^{2+}$	0.2127	0.2115	78.4	77.7	0.1389	0.1389	0.1501
2 $[Ru(bpy)_2dpq]^{2+}$	0.2128	0.2116	78.3	77.7	0.1388	0.1388	–
3 $[Ru(bpy)_2dcdpq]^{2+}$	0.2129	0.2116	78.2	77.7	0.1389	0.1389	0.1435

[a] $M–N_m$ expresses the coordination bond length between the metal ion and the main ligand.
[b] A_m expresses the coordination bond angle between the metal ion and the main ligand.
[c] $C–C_m$ ($C–N_m$) expresses the mean bond length of the main ligand skeleton.
[d] $C–C_{co}$ ($C–N_{co}$) expresses the mean bond length of the co-ligand skeleton (including the longest bond linking the two pyridyl rings in bpy).

be reliable for the theoretical study, and these errors can be thought as systemic errors caused by the computation method and environment factors. Therefore, based on the computed geometries of the complexes, the studies on the electronic structures, trend in DNA-binding, and spectral properties of complexes $[Ru(bpy)_2L]^{2+}$ (L = dmdpq, dpq, and dcdpq) with the DFT and TDDFT methods can be further performed.

4.2. Trend in DNA-binding affinities of the complexes and theoretical explanations

The binding constants (K_b) of the complexes to calf thymus DNA were experimentally determined and given also in Table 1.

For $[Ru(bpy)_2L]^{2+}$, the low energy absorption band centered at 450–458 nm (see Fig. 2) in DNA medium can be assigned to metal-to-ligand charge transfer (MLCT) transition [52]. The intrinsic binding constants K_b of complexes **1**–**3** were measured to be 2.3×10^4, 4.7×10^4 and 3.9×10^5 M^{-1}, respectively. Comparing the intrinsic binding constants of the three complexes with those of the so-called DNA-intercalative Ru(II) complexes (1.1×10^4–4.8×10^4 M^{-1}) [54,55], and considering the results reported by us before [44,47], we can deduce that these complexes **1**–**3** all bind to DNA in intercalation mode.

The DNA-binding of the complexes through intercalation usually leads to the change of hypochromism (H%) and bathochromism ($\Delta\lambda$), due to the intercalation mode involving a strong π–π stacking interaction between an aromatic chromophore and the base pairs of DNA. The extent of hypochromism (H%) closely correlates to the DNA-binding affinity of complexes, and the hypochromisms (H%) of **1**–**3** were measured to be −11%, −14% and −20%, respectively. Such a trend is here in agreement with that in the binding constants. On the other hand, luminescence-spectroscopic studies can further confirm the trend in DNA-binding constants of the complexes $[Ru(bpy)_2L]^{2+}$. The relative luminescence strengths (I/I_0) were obtained to be 2.7, 3.2 and 20.7 for complexes **1**–**3**, respectively. This implies that this series of the complexes can intercalate between the base pairs of DNA and thus be protected by DNA efficiently, since the hydrophobic environment inside the DNA helix reduces the accessibility of solvent water molecules to the complex and the complex mobility is restricted at the binding site, leading to the decrease of the vibration modes of relaxation. Such a trend is also in agreement with that in the binding constants (K_b).

The trend in DNA-binding activities of the complexes can be reasonably explained by our theoretical computations with the DFT method and the frontier molecular orbital theory [38,39]. As well-established, there are π–π stacking interactions in the DNA-binding of these complexes in intercalation mode. As above-mentioned, the DNA molecule is generally an electron-donor and the intercalated complex is an electron-acceptor. According to the frontier molecular orbital theory, a higher HOMO energy of DNA molecule and a lower LUMO energy of the complex molecule are more advantageous to the interaction between these two molecules, because "electron-cloud" more easily transfers from the HOMO of the DNA molecule to the LUMO of the complex and then it must result in a stronger interaction between DNA and the complex. Kurita and Kobayashi [37] have reported a simple calculation model and computed results by the DFT method for stacked DNA base-pairs with backbones. It should be a rather reasonable approximation model for DNA, and thus should be useful for such a discussion. The energies of the HOMO and 6 occupied MOs lying near the HOMO for the CG/CG stacking calculated by the authors were −1.27, −1.33, −1.69, −1.79, −1.98, −2.06 and −2.08 eV, respectively, and the components of HOMO and NHOMO were mainly distributed on the base-pairs. We have also performed some calculations for the complexes using the DFT method, and the calculated energies of their LUMOs and unoccupied MOs lying near the LUMOs for $[Ru(bpy)_2L]^{2+}$ are in the range from −7.8 to −4.0 eV, and the components of these MOs distribute predominantly on the ligands, in particular, on the

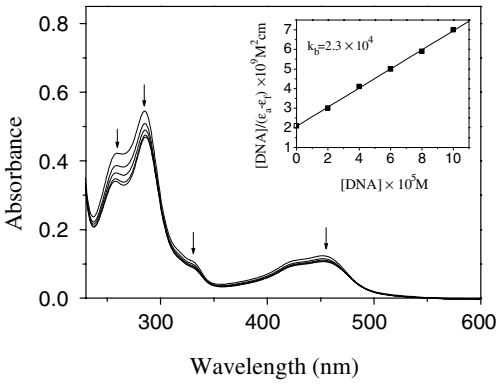

(a) $[Ru(bpy)_2(dmdpq)]^{2+}$ (**1**, $K_b = 2.3 \times 10^4$ M^{-1}).

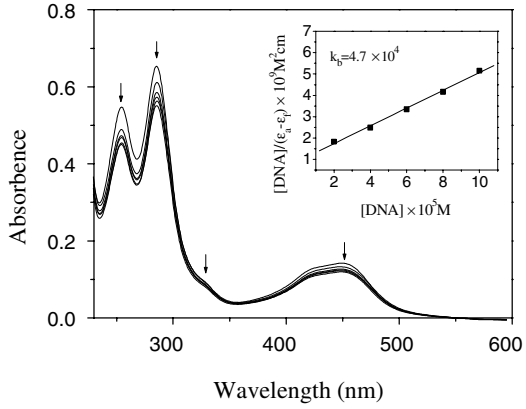

(b) $[Ru(bpy)_2(dpq)]^{2+}$ (**2**, $K_b = 4.7 \times 10^4$ M^{-1}).

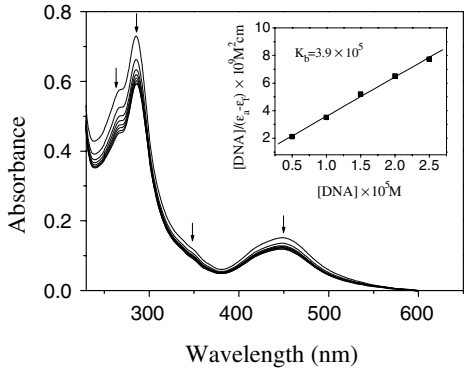

(c) $[Ru(bpy)_2(dcdpq)]^{2+}$ (**3**, $K_b = 3.9 \times 10^5$ M^{-1}).

Fig. 2. Absorption spectra of complexes in 5 mM Tris–HCl and 50 mM NaCl buffer (pH 7.2) in the presence of various amounts of CT-DNA ([DNA] = 0–100 μM, [Ru] = 10 μM).

intercalative ligands. It can be clearly seen that the energies of the HOMO and the occupied orbitals lying near the HOMO of the DNA model are all much higher than those of the LUMO and many unoccupied MOs lying near the LUMO of each one of $[Ru(bpy)_2L]^{2+}$. Therefore, these complexes should all be good electron acceptors in their interactions with DNA and the lower LUMO energy and the predominant LUMO population on the intercalative ligand of the complex should be advantageous to their accepting the electron from base-pairs of DNA. That is to say, the LUMO energies as well as the LUMO populations on the intercalative ligands of the complexes should be very important factors correlating to their DNA-binding constants K_b of the complexes. In addition, the planarity area (S) of intercalative ligand of the metal complex is also surely an important factor, because the larger the planarity area (S) of the intercalative ligand is, the more the binding sites are, and thus the stronger the π–π interaction between intercalative ligand and base-pairs of DNA is.

The experimental results show that the trend in DNA-binding constants (K_b) is $K_b(\mathbf{3}) > K_b(\mathbf{2}) > K_b(\mathbf{1})$. It can be attributed to the sequence of LUMO energies of the complexes (see in Table 3 or Fig. 3), i.e., $\varepsilon_L(\mathbf{3}) < \varepsilon_L(\mathbf{2}) < \varepsilon_L(\mathbf{1})$, since the planarity areas (S) of intercalative ligands of these complexes are almost equal.

It is notable that our experiments also show the constant K_b (3.9×10^5 M^{-1}) of **3** to be much greater than those of **1** and **2**, shown in Table 1 and Fig. 2. Such a trend can also be clearly explained from our theoretical results. As above-mentioned, the substituent –CN with strong withdrawing ability can make not only the LUMO energy of the corresponding substitution derivative lower but also its LUMO components predominantly be distributed on the intercalative ligand, shown in Fig. 4 [**3**, LUMO (3b)]. On the contrary, the LUMO components of **1** and **2** are distributed predominantly on the co-ligands, and just only a little on the intercalative ligand. Therefore, it can be expected that the interaction between the intercalative ligand of **3** and the base pairs of DNA should be much stronger due to the direct contact between its LUMO and the HOMO (and NHOMO) of DNA base-pair model. This is also why the DNA-binding constant of **3** is much greater.

This trend suggests that the DNA-binding affinities of the complexes can be effectively controlled by selecting a suitable substituent via a consideration of both the energies and populations of the LUMOs (perhaps, and NLUMOs) of the substitution derivatives when the planarity areas (S) of their intercalative ligands are almost equal.

4.3. Spectral properties of the complexes and the theoretical explanations

As well-established, the lowest energy electron-transfer spectra of such a type of Ru(II) complexes are assigned to ^{1}MLCT spectra. Since such spectra play a very important role in the study of interaction between a complex and DNA, it is necessary and significant to theoretically clarify the detail of the spectra. The

Table 3
Symmetries and energies (ε_i/a.u.) of some frontier molecular orbitals of $[Ru(bpy)_2L]^{2+}$ (1a.u. = 27.21 eV)

No.	Point group	Occ[a]	Occ	NHOMO	HOMO	LUMO	NLUMO	Vir[b]	$\Delta\varepsilon_{L-H}$
1	C_2	1a	2a	1b	3a	2b	4a	3b	
		−0.4153	−0.4062	−0.4030	−0.3999	−0.2680	−0.2655	−0.2596	0.1319
2	C_2	1a	2a	1b	3a	2b	4a	3b	
		−0.4275	−0.4105	−0.4088	−0.4046	−0.2716	−0.2689	−0.2660	0.1330
3	C_2	1b	1a	2b	2a	3b	3a	4b	
		−0.4465	−0.4205	−0.4194	−0.4145	−0.2857	−0.2802	−0.2794	0.1288

[a] Occ: occupied molecular orbital; HOMO (or H): the highest Occ; NHOMO (or NH): the next HOMO (or HOMO − 1).
[b] Vir: virtual molecular orbital; LUMO (or L): the lowest Vir; NLUMO (or NL): the next LUMO (or LUMO + 1).

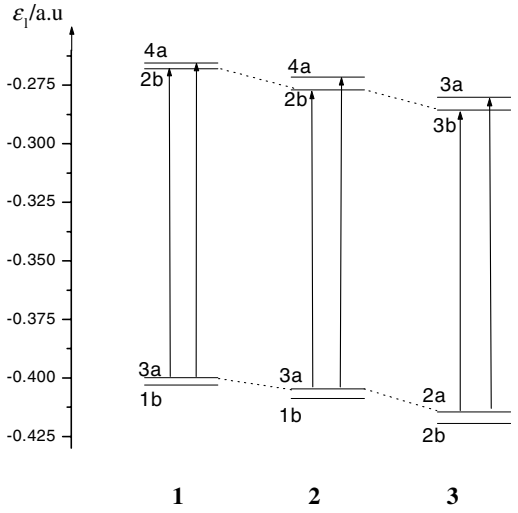

Fig. 3. Schematic representation of energies and the related energy transitions of some frontier molecular orbitals of $[Ru(bpy)_2L]^{2+}$.

TDDFT approach is a very good tool for computing the wavelengths and revealing the spectral properties of the complexes. The computed compositions of some frontier molecular orbitals of the complexes are given in Table 4, and their theoretical wavelengths and properties of the ^{1}MLCT are given in Table 5. The experimental absorption-spectral data are also listed to compare with the results of the TDDFT calculations in Table 5. We can see that the computed wavelengths are well in accordance with the corresponding experimental data. However, it is very important to further reveal the difference of spectral properties in detail with the TDDFT calculations.

The charge-transfer of transition metal complex can be traditionally classified into three categories: (i) a metal-to-ligand (MLCT), (ii) a ligand-to-ligand (LLCT), and (iii) a ligand-to-metal (LMCT). From Table 4, we can see that the HOMOs of $[Ru(bpy)_2L]^{2+}$ are all characteristic of metal–ligand orbital (~83% metal d-orbital and ~17% ligand π-orbital), whereas the LUMOs are all predominantly characteristic of ligand-π*-orbitals. However, it is notable that the LUMO (and some unoccupied orbitals near LUMO) of complex **3** is predominantly distributed on main ligand (dcdpq), whereas those of complexes **1** and **2** are predominantly distributed on co-ligand (bpy) although mixed with π*-orbitals of main ligand to a certain extent.

TDDFT is based on linear-response theory and is structurally similar to CIS (configuration interaction using single excitations), but yields better results due to the use of the Kohn–Sham exchange and correlation potential [22,23]. The calculated linear combination coefficients of configurations for the lowest singlet excited states of the complexes are given in Table 5. Combining them with the molecular orbital composition characteristic (contribution column) offered from Table 4, the electron transfer characteristic of the lowest excited states can be assigned (see the last column in Table 5). Since the lowest singlet excited states of complexes **1** and **2** mainly correspond to a transfer from HOMO to LUMO + 1 (H_0 to L_1) with coefficient (coef.) being 0.69, their corresponding spectra can be assigned as ^{1}MLCT ($d_{Ru} \rightarrow \pi^*_{bpy}$) in a spectral property. However, the lowest singlet excited state of complex **3** is quite different from those of complexes **1** and **2**, because it mainly corresponds to a transfer (H_0 to L_0, coef. = 0.53) including a transfer (H_0 to L_3, coef. = −0.42) and its corresponding spectrum can be assigned to ^{1}MLCT ($d_{Ru} \rightarrow \pi^*_{dcdpq}$). Such differences can owe to the substituent effects. The substituent (–CN) with strong electron-withdrawing ability can reduce the negative charge density of dpq of the intercalative ligand (dcdpq), and thus the d-orbital electron of Ru can easily transfer to the intercalative ligand (dcdpq). On the contrary, the substituent $-CH_3$ with strong electron-pushing ability can increase the negative charge density of dpq of the intercalative ligand (dmdpq), and thus the d-orbital electron of Ru can easily transfer to the co-ligand (bpy), not to the intercalative ligand (dmdpq).

Although TDDFT calculations in the spectra of many complexes are reliably accurate for both wavelengths and spectral properties, it is still a simple and effective analytic method in the above-spectral explanation to apply the frontier molecular orbital theory based on the general DFT calculations. The computed stereo-contour graphs of HOMO, LUMO and NLUMO of the complexes with the general DFT method are shown in

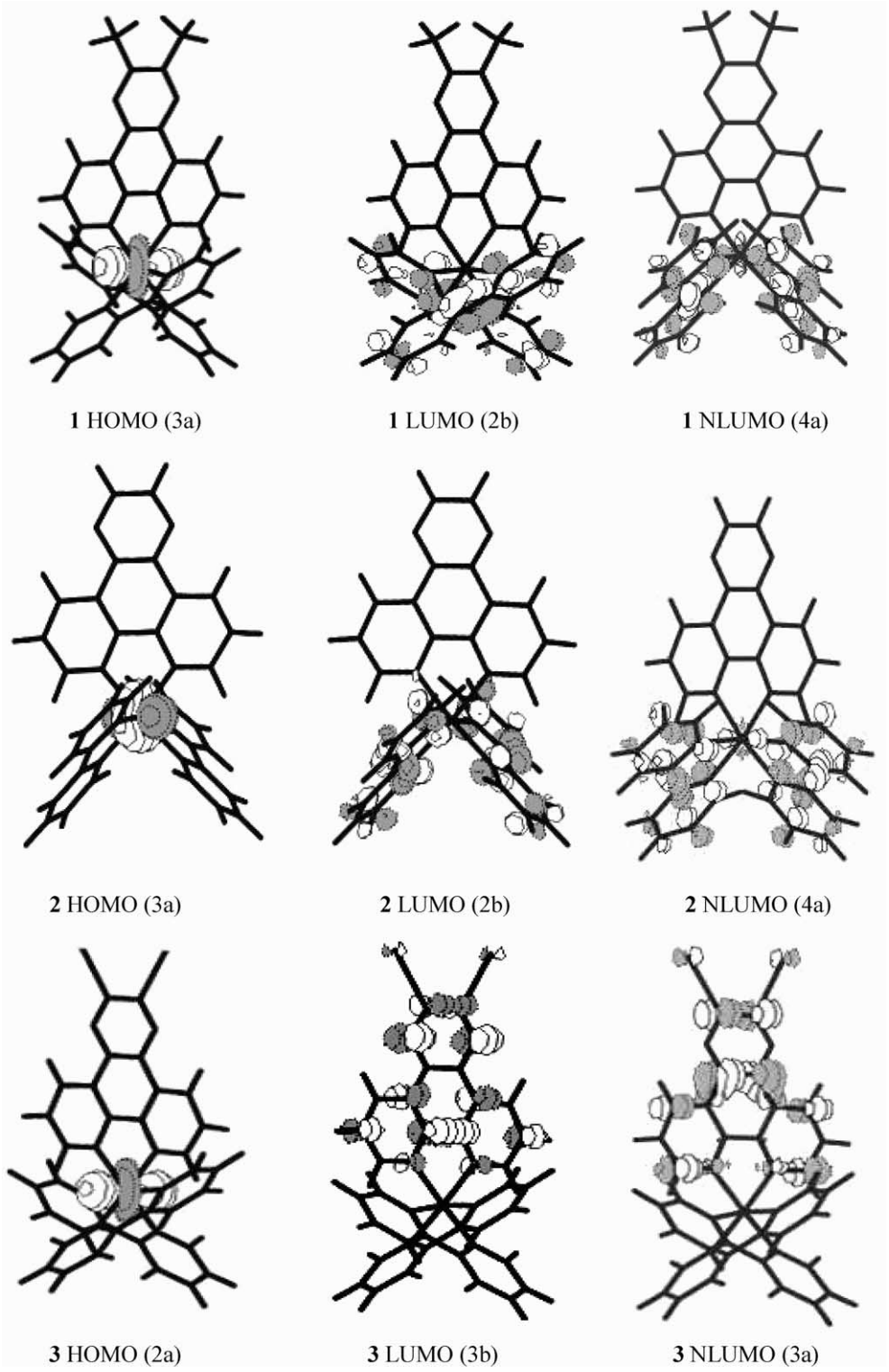

Fig. 4. Stereo-contour graphs of HOMOs and LUMOs of $[Ru(bpy)_2L]^{2+}$.

Fig. 4. From Fig. 4, we can easily see that: the HOMOs of the three complexes are all essentially characteristic of d-orbitals of Ru ion (d_{Ru}); the LUMOs (and LUMOs + 1) of complexes **1** and **2** are predominantly characteristic of π*-orbitals of co-ligand (π^*_{bpy}) and the LUMO (and LUMO + 1) of complex **3** is predominantly characteristic of π*-orbitals of main-ligand (π^*_{dcdpq}). Therefore, the above-mentioned spectral properties (^{1}MLCT) for the lowest energy bands can also be reasonably explained. On the other hand, the wavelength

Table 4
Orbitals involved in the description of the lowest singlet excited states of $[Ru(bpy)_2L]^{2+}$

$[Ru(bpy)_2(dmdpq)]^{2+}$ (**1**)			$[Ru(bpy)_2(dpq)]^{2+}$ (**2**)			$[Ru(bpy)_2(dcdpq)]^{2+}$ (**3**)		
Orbital	Label	Contribution	Orbital	Label	Contribution	Orbital	Label	Contribution
LUMO + 1	L_1	7% d_{Ru} 92% π^*_{bpy} 1% π^*_{dmdpq}	LUMO + 1	L_1	7% d_{Ru} 92% π^*_{bpy} 1% π^*_{dpq}	LUMO + 3	L_3	7% d_{Ru} 31% π^*_{bpy} 62% π^*_{dcdpq}
LUMO	L_0	3% d_{Ru} 93% π^*_{bpy} 4% π^*_{dmdpq}	LUMO	L_0	2% d_{Ru} 89% π^*_{bpy} 9% π^*_{dpq}	LUMO + 2	L_2	2% d_{Ru} 65% π^*_{bpy} 33% π^*_{dcdpq}
HOMO	H_0	83% d_{Ru} 11% π_{bpy} 6% π_{dmdpq}	HOMO	H_0	83% d_{Ru} 11% π_{bpy} 6% π_{dpq}	LUMO + 1	L_1	1% d_{Ru} 6% π^*_{bpy} 93% π^*_{dcdpq}
						LUMO	L_0	1% d_{Ru} 3% π^*_{bpy} 96% π^*_{dcdpq}
						HOMO	H_0	84% d_{Ru} 11% π_{bpy} 5% π_{dcdpq}

Table 5
Calculated energies and the assignments of the lowest singlet excited states of $[Ru(bpy)_2L]^{2+}$

No.	Complex	Wavelength (nm)		Principal excitation	Coefficient	Assignment
		Calc.	Expt.			
1	$[Ru(bpy)_2(dmdpq)]^{2+}$	455	453	$H_0 \rightarrow L_1$	0.69	$d_{Ru} \rightarrow \pi^*_{bpy}$
2	$[Ru(bpy)_2(dpq)]^{2+}$	449	453	$H_0 \rightarrow L_1$	0.69	$d_{Ru} \rightarrow \pi^*_{bpy}$
3	$[Ru(bpy)_2(dcdpq)]^{2+}$	455	450	$H_0 \rightarrow L_0$	0.53	$d_{Ru} \rightarrow \pi^*_{dpq}$
				$H_0 \rightarrow L_3$	−0.42	$d_{Ru} \rightarrow \pi^*_{dpq,bpy}$

calculations from the energy difference ($\Delta\varepsilon_{L-H}$) between the LUMO and HOMO of the complex on an absolute sense are not rather accurate and greater than the corresponding energies (ΔE) of the ^{1}MLCT absorption spectra of the complexes by 0.75–0.88 eV. However, such an error can be reduced by using a standard sample correction method, i.e., an approximate correlation of reverse ratio of the energy difference ($\Delta\varepsilon_{L-H}$) between the LUMO and the HOMO to experimental wavelength (λ) [40,42], and thus such a simple estimation for the wavelength calculations is still useful in the qualitative spectral analysis.

5. Conclusions

The DNA-binding constants K_b of a series of Ru(II) polypyridyl complexes $[Ru(bpy)_2L]^{2+}$ (L = dmdpq, dpq, and dcdpq) were determined systematically with spectrophotometric titration. The experimental results show that these complexes bind to DNA in intercalation mode, and the order of their intrinsic DNA-binding constants K_b is $K_b(\mathbf{1}) < K_b(\mathbf{2}) \ll K_b(\mathbf{3})$. The substituents on the intercalative ligands of the complexes play a very important role in the control of DNA-binding affinities of the complexes, in particular, the stronger electron-withdrawing substituent (–CN) on the intercalative ligand can greatly improve the DNA-binding property of the derivative complex. The trend in DNA-binding affinities of this series of complexes can be reasonably explained by applying the DFT method and the frontier molecular orbital theory, and it suggests that the DNA-binding affinities of the complexes can be effectively controlled by selecting a suitable substituent to change the energy and population of the LUMO (and NLUMO) of the substitution derivative. In addition, the spectral properties of the complexes can further be discussed by applying the TDDFT method.

Acknowledgments

We are grateful to the supports of the National Natural Science Foundation of China, the Research Fund for the Doctoral Program of Higher Education, the Natural Science Foundation of Guangdong Province, and the State Key Laboratory of Coordination Chemistry in Nanjing University.

References

[1] M.J. Clarke, Coord. Chem. Rev. 236 (2003) 209.
[2] L.-N. Ji, X.-H. Zou, J.-G. Liu, Coord. Chem. Rev. 216–217 (2001) 513.

[3] M.K. Nazeeruddin, S.M. Zakeeruddin, R. Humphry-Baker, S.I. Gorelsky, A.B.P. Lever, M. Gratzel, Coord. Chem. Rev. 208 (2000) 213.
[4] O. Novalova, H. Chen, O. Vrana, A. Rodger, P.J. Sadler, V. Brabec, Biochemistry 42 (2003) 11544.
[5] L.M. Wilhelmsson, F. Westerlund, P. Lincoln, B. Norden, J. Am. Chem. Soc. 124 (2002) 12092.
[6] A. Hergueta-Bravo, M.E. Jimenez-Hernandez, F. Montero, E. Oliveros, G. Orellana, J. Phys. Chem. B 106 (2002) 4010.
[7] C. Moucheron, A.K.-D. Mesmaeker, J. Phys. Org. Chem. 11 (1998) 577.
[8] L. Mishra, A.K. Yadaw, S. Srivastava, A.B. Patel, New J. Chem. 24 (2000) 505.
[9] W.-J. Mei, J. Liu, K.-C. Zheng, L.-J. Lin, H. Chao, A.-X. Li, F.-C. Yun, L.-N. Ji, Dalton Trans. (2003) 1352.
[10] L. Mishra, R. Sinha, H. Itokawa, K.F. Bastow, Y.Y. Tachibana, Y. Nakanishi, N. Kilgore, K.H. Lee, Bioorg. Med. Chem. 9 (2001) 1667.
[11] Q.-X. Zhen, B.-H. Ye, J.-G. Liu, Q.-L. Zhang, L.-N. Ji, L. Wang, Inorg. Chim. Acta 303 (2000) 141.
[12] D.Z.M. Coggan, I.S. Haworth, P.J. Bates, A. Robinson, A. Rodger, Inorg. Chem. 38 (1999) 4486.
[13] R.R. Ruminski, P.T. Deere, M. Olive, D. Serveiss, Inorg. Chim. Acta 281 (1998) 1.
[14] P. Lincoln, A. Broo, B. Norden, J. Am. Chem. Soc. 118 (1996) 2644.
[15] R.M. Hartshorn, J.K. Barton, J. Am. Chem. Soc. 114 (1992) 5919.
[16] P. Lincoln, B. Norden, J. Phys. Chem. B 102 (1998) 9583.
[17] Y. Xiong, L.-N. Ji, Coord. Chem. Rev. 185–186 (1999) 711.
[18] P. Yang, D.-X. Han, Z.-H. Xiong, J. Mol. Struct. (Theochem.) 540 (2001) 211.
[19] P. Hohenberg, K. Kohn, Phys. Rev. B 106 (1964) 864.
[20] D. Becke, J. Chem. Phys. 98 (1993) 1372.
[21] A. Gorling, Phys. Rev. 54 (1996) 3912.
[22] J.B. Foresman, Æ. Frisch, Exploring Chemistry with Electronic Structure Methods, second ed., Gaussian, Inc., Pittsburgh, PA, 1996.
[23] I. Frank, SIMU Newsletter 3 (2001) 61.
[24] P.J. Hay, J. Phys. Chem. A 106 (2002) 1634.
[25] L. Ghizdavu, O. Lentzen, S. Schumm, A. Brodkorb, C. Moucheron, A.K. Mesmaeker, Inorg. Chem. 42 (2003) 1935.
[26] G. Pourtois, D. Beljonne, C. Moucheron, S. Schumm, A.K.-D. Mesmaeker, R. Lazzaroni, J.-L. Bredas, J. Am. Chem. Soc. 126 (2004) 683.
[27] N.H. Damrauer, B.T. Weldon, J.K. McCusker, J. Phys. Chem. A 102 (1998) 3382.
[28] P. Brandt, T. Norrby, B. Akermark, Inorg. Chem. 37 (1998) 4120.
[29] R. Salzmann, C.J. Ziegler, N. Godbout, M.T. Mcmahon, K.S. Suslick, E. Oldfield, J. Am. Chem. Soc. 120 (1998) 11323.
[30] A. Voigt, U. Abram, R. Bottcher, U. Richter, J. Reinhold, R. Kirmse, Chem. Phys. 253 (2000) 171.
[31] S. Tobisch, T. Nowak, H. Bögel, J. Organmet. Chem. 619 (2001) 21.
[32] M.J. Bakker, F.W. Vergeer, F. Hartl, P. Rosa, L. Ricard, P.L. Floch, M.J. Calhorda, Chem. Eur. J. 8 (2002) 1741.
[33] J.F. Guillemoles, V. Barone, L. Joubert, C. Adamo, J. Phys. Chem. A 106 (2002) 11354.
[34] T. Megyes, G. Schubert, M. Kovacs, T. Radnet, T. Grosz, I. Bako, I. Papai, P. Horvath, J. Phys. Chem. A 107 (2003) 9903.
[35] S.R. Stoyanov, J.M. Villegas, D.P. Rillema, Inorg. Chem. 41 (2002) 2941.
[36] D. Reha, M. Kabelac, F. Ryjacek, J. Sponer, J.E. Sponer, M. Elstner, S. Suhai, P. Hobza, J. Am. Chem. Soc. 124 (2002) 3366.
[37] N. Kurita, K. Kobayashi, Comput. Chem. 24 (2000) 351.
[38] K. Fukui, T. Yonezawa, H. Shingu, J. Chem. Phys. 20 (1952) 722.
[39] I. Fleming, Frontier Orbital and Organic Chemical Reaction, Wiley, New York, 1976.
[40] K.-C. Zheng, J.-P. Wang, W.-L. Peng, X.-W. Liu, F.-C. Yun, J. Phys. Chem. A 105 (2001) 10899.
[41] K.-C. Zheng, X.-W. Liu, J.-P. Wang, F.-C. Yun, L.-N. Ji, J. Mol. Struct. (Theochem.) 637 (2003) 195.
[42] K.-C. Zheng, J.-P. Wang, W.-L. Peng, Y. Shen, F.-C. Yun, Inorg. Chim. Acta 328 (2002) 247.
[43] Jie Liu, W.-J. Mei, L.-J. Lin, K.-C. Zheng, Hui Chao, F.-C. Yun, L.-N. Ji, Inorg. Chim. Acta 357 (2004) 285.
[44] Q.-X. Zhen, B.-H. Ye, J.-G. Liu, L.-N. Ji, Chem. J. Chin. Univ. 20 (1999) 1661.
[45] C.A. Zwelling, S. Michaels, H. Schwarts, P.P. Dobson, K.W. Kohn, Cancer Res. 41 (1981) 460.
[46] A. Ambroise, B.G. Maiya, Inorg. Chem. 39 (2000) 4264.
[47] L. Wang, H.-Y. Zhou, J.-Y. Wang, T.-X. Zeng, L.-N. Ji, Chin. Chem. Lett. 6 (1995) 353.
[48] A. Wolfe, G.H. Shimer, T. Mechan, Biochemistry 26 (1987) 6392.
[49] M.J. Frisch, G.W. Trucks, H.B. Schlegel, G.E. Scuseria, M.A. Robb, J.R. Cheeseman, V.G. Zakrzewski, J.A. Montgomery, R.E. Stratmann, J.C. Burant, S. Dapprich, J.M. Millam, A.D. Daniels, K.N. Kudin, M.C. Strain, O. Farkas, J. Tomasi, V. Barone, M. Cossi, R. Cammi, B. Mennucci, C. Pomelli, C. Adamo, S. Clifford, J. Ochterski, G.A. Petersson, P.Y. Ayala, Q. Cui, K. Morokuma, D.K. Malick, A.D. Rabuck, K. Raghavachari, J.B. Foresman, J. Cioslowski, J.V. Ortiz, A.G. Baboul, B.B. Stefanov, G. Liu, A. Liashenko, P. Piskorz, I. Komaromi, R. Gomperts, R.L. Martin, D.J. Fox, T. Keith, M.A. Al-Laham, C.Y. Peng, A. Nanayakkara, M. Challacombe, P.M.W. Gill, B. Johnson, W. Chen, M.W. Wong, J.L. Andres, C. Gonzalez, M. Head-Gordon, E.S. Replogle, J.A. Pople, GAUSSIAN-98, Revision A.11.4, Gaussian, Inc., Pittsburgh, PA, 2002.
[50] P.J. Hay, W.R. Wadt, J. Chem. Phys. 82 (1985) 277.
[51] W.R. Wadt, P.J. Hay, J. Chem. Phys. 82 (1985) 284.
[52] A. Juris, V. Balzani, F. Barigelletti, S. Campagna, P. Belser, A.V. Zelewsky, Coord. Chem. Rev. 84 (1988) 85.
[53] G. Schaftenaar, J.H. Noordik, J. Comput. Aided Mol. Design 14 (2000) 123.
[54] A.M. Pyle, J.P. Rehmann, R. Meshoyrer, C.V. Kumar, N.J. Turro, J.K. Barton, J. Am. Chem. Soc. 111 (1989) 3051.
[55] X.-H. Zou, B.-H. Ye, H. Li, Q.-L. Zhang, H. Cao, J.-G. Liu, L.-N. Ji, X.-Y. Li, J. Biol. Inorg. Chem. 6 (2001) 143.